Original Article

New polyketides from Liuweizhiji Gegen-Sangshen oral liquid and their anti-inflammatory, hepatoprotective activities *in-vitro,* and molecular docking analysis

Mengyu Zhang[a], Baorui Teng[a], Xin Zhou[b], Dan Zhang[a], Xiujuan Fu[a], Siwei Chen[a], Sijing Liu[c], Zhi Li[b,*], Hui Lei[a,d,*]

[a]Department of School of Pharmacy, Southwest Medical University, Luzhou, China
[b]Department of Spleen and Stomach Diseases, the Affiliated Traditional Chinese Medicine Hospital of Southwest Medical University, Southwest Medical University, Luzhou, China
[c]Department of Pharmacy, The Second People's Hospital of Deyang, Deyang, Sichuan, China
[d]Daniel K. Inouye College of Pharmacy, University of Hawaii at Hilo, Hilo, United States

ARTICLE INFO

ABSTRACT

Liuweizhiji Gegen-Sangshen (LGS) oral liquid, a commercially available health product in China, has attracted extensive attention due to its application in treatment of alcoholic liver disease. Whereas, no studies on the chemical composition of LGS have been reported. In this work, two new polyketide compounds (**1**, **2**), and ten known compounds (**3-12**) were purified and identified from LGS oral liquid whose structures were illuminated by detailed NMR, MS, and ECD calculations. The anti-inflammatory and hepatoprotective activities of isolated monomers were tested. Compounds **2** and **3** reduced the content of NO induced by LPS, with IC_{50} values of 83.6±0.54 μM and 32.5±0.73 μM, respectively. The optimal bioactivity evaluations and molecule docking results showed that compound **3** had the potential to be developed as a lead drug with anti-inflammatory activity. In addition, compounds **1**, **4**, and **9** alleviated alcohol-induced damage to human hepatic L02 cells and reduced the release of ALT and AST, indicating that these compounds possess good hepatoprotective activity for the treatment of ALD. Furthermore, the possible pathway for the biosynthesis of compound **2** were also hypothesized.

1. Introduction

Alcoholic liver disease (ALD) is the most prevalent liver disease across many countries, mainly caused by long-term or excessive drinking, with pathological features such as metabolic disorders, inflammation, and fibrosis [1]. In ALD progression, alcohol activates Kupffer cells, induces NF-κB activation, and promotes the release of inflammatory cytokines such as TNF-α and IL-6, driving liver fibrosis. Excessive nitric oxide (NO) production mediated by inducible nitric oxide synthase (iNOS) exacerbates hepatocyte damage, not only leading to oxidative stress but also aggravating hepatocyte apoptosis through nitration of proteins and DNA damage. Therefore, inhibition of the overexpression of inflammatory biomarkers becomes a key target for intervening in ALD [2,3]. The L02 human normal hepatocyte cell line, due to its stable proliferative capacity and sensitivity to ethanol-induced damage, is widely used for the construction of *in-vitro* models of ALD [4,5]. By stimulating L02 cells with ethanol, the characteristics of hepatic metabolic disorder, lipid peroxidation, and inflammatory cytokine release observed in ALD can be mimicked, providing a reliable platform for evaluating the protective effects of drugs. When hepatocytes are damaged, the permeability of the cell membrane increases, leading to the release of aspartate aminotransferase (AST) and alanine aminotransferase (ALT) from the hepatocytes. Therefore, AST

and ALT are selected as characteristic and highly sensitive indicators for assessing the degree of liver function impairment.

During the past decades, polyene phosphatidylcholine, phosphodiesterase inhibitors, and glucocorticoids, were used as common treatments for alcoholic liver injury in clinics [6-9]. However, long-term use of these drugs causes resistance or significant side effects [10]. Numerous reports and studies have demonstrated that natural active components, such as flavonoids, terpenes, and polyphenols, can alleviate ALD [11-13]. Therefore, it is of great significance to research safe, natural, and effective drugs or precursors from plant-based ingredients or functional foods for treating ALD.

Liuweizhiji Gegen-Sangshen oral liquid (LGS), a commercially available health product including six types of homologous substances of medicine and food, enthusiastically used in China, possesses a wide spectrum of pharmacological properties [14,15], such as strengthening the spleen and promoting dampness and blood circulation, possessing anti-liver cancer activity, relieving hepatotoxicity, and preventing ALD [16,17]. Current studies on LGS mostly cast upon crude extraction; however, until now, very little has been known about its active ingredients or pharmacologic mechanisms [18]. Especially, the overall chemical components of the LGS formulation are still unknown. Therefore, it is essential to systematically study the chemical diversity of LGS.
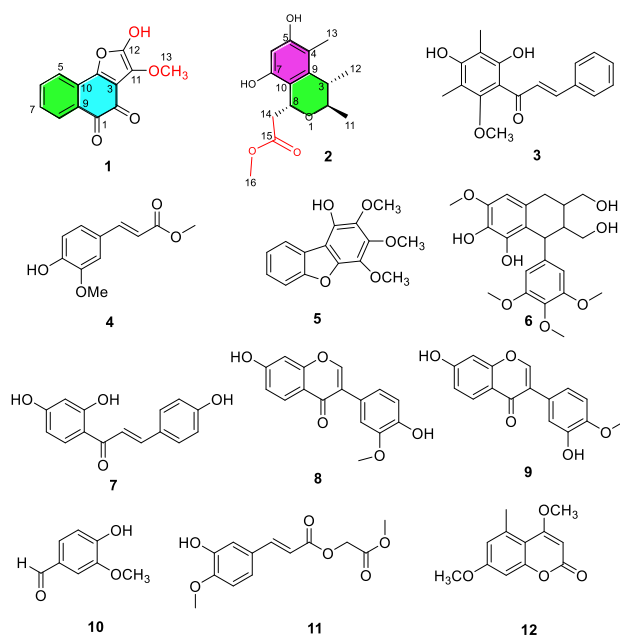
Figure 1. Chemical structures of compounds 1-12.

Table 1. ^{1}H NMR (400 MHz) and ^{13}C NMR (100 MHz) data for compounds **1** and **2** in CD$_3$OD.

No.	1		2	
	d_C, type	d_H (*J* in Hz)	d_C, type	d_H (*J* in Hz)
1	180.7, C	-	-	-
2	175.3, C	-	75.7, CH	3.72, dd (6.8,3.3)
3	152.5, C	-	36.9, CH	2.63, dd (6.8,3.2)
4	158.0, C	-	114.0, C	-
5	113.8, CH	7.71, d (8.0)	156.1, C	-
6	130.1, CH	7.58, t (8.0)	101.4, CH	6.10, s
7	127.1, CH	7.49, t (8.0)	152.6, C	-
8	124.0, CH	8.09, dt (8.0)	70.6, CH	5.07, dd (10.1, 3.7)
9	123.5, C	-	139.5, C	-
10	121.2, C	-	114.2, C	-
11	146.8, C	-	22.2, CH$_3$	1.19, d (6.8)
12	148.2, C	-	20.7, CH$_3$	1.01, d (6.8)
13	62.1, OCH$_3$	4.03, s	10.9, CH$_3$	1.94, s
14			42.7, CH$_2$	3.43, dd (15.1,3.7) 2.35, dd (15.1,10.1)
15			175.0, C	-
16			52.1, OCH$_3$	3.58, s

As part of our continuing endeavor to search for effective drugs or precursors for treating ALD from natural products, an extract of LGS was investigated. This study discovered two new polyketide compounds (**1**, **2**) and ten known compounds (**3-12**) (Figure 1). Herein, we present a comprehensive account of the structural elucidation of these novel compounds, leveraging spectroscopic analyses, MS data, and electronic circular dichroism (ECD) calculations. Additionally, we evaluated the anti-inflammatory and hepatoprotective activities of isolated compounds. Furthermore, the possible biosynthetic pathway for compound **2** was also postulated.

2. Materials and Methods

2.1. General experimental procedures

HRESIMS, IR, and Ultraviolet (UV) spectra were processed on a Bruker maXis TOF-Q mass, a Shimadzu IR spectrometer, and a UV-2550 spectrophotometer, respectively. NMR spectra were recorded using Magnet System 400 (Bruker) and Avance III-600 (Bruker) using the tetramethylsilane (TMS) peak used as the internal standard. Sephadex LH-20 (MeOH), and silica gel were carried out on column chromatography (CC). Preparative HPLC was prepared by a SAIPURUISHE system equipped with a UV absorbance detector and octadecylsilyl silica (ODS) column.

2.2. Plant material

The source of commercial liuweizhiji gegen-sangshen (LGS) oral liquid has been mentioned in the previous paper [16].

2.3. Extraction and isolation

LGS was diluted with water and subsequently extracted with ethyl acetate to obtain a crude extract. This extract was then concentrated to yield a semisolid paste for further purification. The ethyl acetate extract (66 g) was processed through silica gel (300-400 mesh) CC, using gradient elution with DCM/ CH$_3$OH (3:0 to 0:1) to collect 11 fractions (Fr.a to Fr.k). Fr.b (131 mg) was processed by silica gel (500-800 mesh) CC with a PE /EtOAc gradient elution (70:1 to 1:1) to obtain five subcomponents, one of which was processed through reverse-phase chromatography using methanol/water (CH$_3$OH/H$_2$O, 75:25) as the eluent to get compound **1** (1.1 mg) and compound **5** (1.2 mg). Fraction Fr.c (169 mg) was processed through normal pressures silica gel (300-400 mesh) CC with a PE / EtOAc eluent (60:1 to 1:1) resulting in seven

subcomponents (Fr.c-1 to Fr.c-7). Fr.c-3 was applied on the preparative HPLC using methanol/water (CH$_3$OH: H$_2$O, 60:40) giving compound **10** (1.9 mg). Fr.c-5 was exposed to preparative HPLC (CH$_3$OH: H$_2$O, 68:32) to afford compound **12** (1.7 mg). Fr.c-6 was purified under similar conditions (CH$_3$OH/H$_2$O, 45:55) to acquire compound **11** (1.9 mg). Fr.e (500 mg) was applied on silica gel CC with a CH$_2$Cl$_2$/ CH$_3$OH gradient (70:1 to 0:1) and further isolated by preparative HPLC (CH$_3$OH/H$_2$O, 56:44) to get compounds **7** (3.1 mg), **8** (2.9 mg), and **9** (2.3 mg). Fr. f was purified by Sephadex LH-20 (CH$_2$Cl$_2$-CH$_3$OH) and next by preparative HPLC (CH$_3$OH: H$_2$O, 65:35) to yield **6** (9.0 mg). Fr.g was processed through a silica gel (PE/AC, 20:1 to 1:1) CC and followed by preparative HPLC (CH$_3$OH: H$_2$O, 60:40) to get compounds **2** (1.2 mg), **3** (1.1 mg), and **4** (2 mg).

2.4. Compound characterization

Compound (**1**): yellow acicular crystal; UV (MeOH) λ$_{max}$ (log ε) 244 (3.24), 320 (3.70) nm; ^{1}H, ^{13}C NMR data (Table 1); HR-MS *m/z* 262.0784 [M+NH$_4$]$^+$ (calcd for C$_{13}$H$_8$NH$_4$O$_5$, 262.0763).

Compound (**2**): white solid; UV (MeOH) λ$_{max}$ (log ε) 254 (3.48) nm; ^{1}H,^{13}C NMR data (Table 1); HR-MS *m/z* 281.1394 [M+H]$^+$ (calcd for C$_{15}$H$_{21}$O$_5$, 281.1376).

2.5. NMR calculations

The conformational searches for compound **2** were conducted using the SYBYL X 2.1.1 program, employing an MMFF94s molecular force field. Subsequently, we optimized all conformers at the B3LYP/6-31+G(d) level. These stable, optimized conformers were further conducted to ECD calculations in methanol. The ECD spectra of compound **2** were then weighted according to the Boltzmann distribution and compared with experimental spectra. The calculation of ECD spectra was performed using SpecDis 1.71 software with a σ value of 0.3 eV.

2.6. Inhibition of NO production assays

We evaluated the inhibitory activity of **1-12** against LPS-activated NO production in RAW 264.7 cells at various concentrations (1, 2, 5, 10, 20, 40, 60, and 100 μM), with dexamethasone serving as the positive control. The assay procedure followed the protocol detailed in a previously published paper [19].

2.7. Molecular docking

To investigate the interaction of compounds **2** and **3** with iNOS, molecular docking was employed by AutoDock Vina 1.1.2 [20], using the method reported in the literature [21].

2.8. Hepatoprotective activities in-vitro of isolated compounds

2.8.1. Establishment of alcohol-induced hepatocyte injury model

L02 cells were incubated into 96-well plates (5×10^3 cells per well). After cell adhesion, the original medium was discarded, and 100 μL ethanol solution with different concentrations (0%, 2%, 2.5%, 3%, 4%, 5%) was added for incubation for 24 hrs. Methylthiazol-2-yl-2,5-diphenyltetrazolium bromide (MTT) assay was used to measure cell viability, calculated as follows (Eq. 1):

$$\text{Cell viability (\%)} = (A - A_0) / (A_1 - A_0) \times 100, \quad (1)$$

where A corresponds to the absorbance value of the experimental group, A_1 corresponds to the absorbance of the control group, and A_0 corresponds to the absorbance of the blank group (containing no cells). The appropriate concentration of ethanol was selected for further experiments.

2.8.2. Effects of the purified compounds on growth of L02 cells

To investigate the potential of the isolated and purified compounds in mitigating excessive cell death in L02 hepatocytes or enhancing the survival rate, we intervened with these compounds at various concentrations. The aim was to identify effective compounds and their appropriate concentration ranges, which could then be further applied to mitigate alcohol-induced damage in L02 hepatic cells.

2.8.3. Effects of different mass concentrations of compounds on alcohol-induced injury in L02 cells

Compounds with cell viabilities exceeding 90% for hepatocyte L02 were screened out, and their effects on ethanol-induced hepatocyte L02 were further explored within the safe concentration range. L02 hepatocytes were cultured with 5% CO_2 at 37°C. In this experiment, cell suspensions in the logarithmic growth phase were plated into 96-well plates at 4×10^3 cells per well and cultured until the cell density reached 50%–60%. The control group received medium without ethanol, the model group was exposed to medium containing ethanol, and the experimental groups were treated with medium containing ethanol and different concentration gradients of the compounds. Each group was set up with 6 replicate wells and incubated for 24 hrs. The MTT method was used to measure absorbance values at 570 nm, which were then utilized to calculate the survival rate.

2.8.4. Measurement of ALT and AST release in alcohol-induced L02 cells

L02 cells were plated into 6-well plates (2.5×10^5 cells per well). The experimental setup included a control group, a model group, a positive control group (bifendate, 10 μg/mL), and three groups administered with low, medium and high concentrations of each compound. Following incubation, the levels of ALT and AST in each group's supernatant were determined in accordance with the instructions provided with the assay kits.

2.9. Statistical analysis

All experiments were performed at least three times. Experimental data were expressed as the mean ± standard deviation (SD) and were performed by using IBM SPSS Statistics 17.0 and GraphPad Prism 9.5.1. One-way analysis of variance (one-way ANOVA) was applied to evaluate statistical significance (p < 0.05).

3. Results and Discussion

3.1. Structural elucidation

Compound **1** had a yellow acicular crystal having the molecular formula $C_{13}H_8O_5$, exhibited signals for four aromatic protons at δ_H 7.58

(t, J = 8.0 Hz), 7.49 (t, J = 8.0 Hz), 8.09 (d, J = 8.0 Hz), and 7.71 (d, J = 8.0 Hz) in its ^{1}H NMR spectrum belonging to a 1, 2-bisubstituent benzene. The ^{1}H and ^{13}C NMR data (Table 1), along with the HSQC spectrum, displayed characteristic resonances for one methoxy group, four methines (olefinic), and eight non-proton-bearing carbons (two ketone carbonyls, and six olefinic ones). Based on the aforementioned data, compound **1** was proposed as a 3,4-furo-1,2-naphthoquinone analog with a tricyclic ring system.

The structure of **1** was clarified through heteronuclear multiple bond correlation (HMBC) and Co-relation spectroscopy (COSY) experiments (Figure 2). HMBC from H-5 to C-7, C-9, and C-4, from H-8 to C-6 and C-10, from H-7 to C-5, and C-9, along with COSY correlations from H-5/H-6/H-7/H-8 suggested the structure of **1** with the 1,2-naphthoquinone. In contrast to crataequinone A, compound **1** showed an additional methoxy group. Further correlations originating from H-13(-OCH$_3$) to C-11 (146.8) confirmed that the methoxy group was located at C-11. Thus, the structure of **1** was identified and named as 11-methoxy-12-hydroxy-3,4-furo-1,2-naphthoquinone.

Compound **2** was purified as a white solid with the molecular formula $C_{15}H_{20}O_5$, based on the [M+H]$^+$ ion peak at m/z 281.1394 in the HRESIMS data and ^{13}C NMR. The ^{1}H NMR data (Table 1) displayed signals for an aromatic proton [6.10, (1H, s)], two oxygenated protons [3.72 (1H, dd, J = 6.8 Hz, 3.3 Hz), 5.07 (1H, dd, J = 10.1 Hz, 3.7 Hz)], and three methyl signals [1.19 (3H, d, J = 6.8 Hz), 1.01 (3H, d, J = 6.8 Hz), 1.94 (3H, s)]. The ^{13}C NMR spectrum (Table 1) and HSQC spectra indicated a total of 15 carbons, which were assigned to three methyls, one methylene, one methoxyl, four methines, and six quaternary carbons. In the 2D NMR data, the HMBC correlations (Figure 2) from H-6 (δ_H 6.10) to C-10 (δ_C 114.2), C-7 (152.6), and C-5 (156.1), from H$_3$-13 (1.94) to C-10 (114.2), C-9 (139.5), and C-5 (156.1), formed a benzene cycle (Figure 2). Similarly, the six membered acetal cycle was confirmed by the spin systems of H$_3$-11/H-2/H-3/ H$_3$-12, and the HMBC correlations from H$_3$-12 (δ_H 1.01) to C-9 (139.5), C-2 (75.7), and C-3 (36.9), and from H$_3$-11 (δ_H 1.19) to C-2 (75.7), and C-3 (36.9). In addition, the signals of -CH$_2$COOCH$_3$ moiety at the C-8 position were supported by the HMBC correlations of δ_H 4.42 (3.43/2.35) with C-8 (70.6), and C-15 (175.0) and the ^{1}H-^{1}H COSY correlations of H-8 (δ_H 5.07)/H-14 (δ_H3.43/2.35). In the nuclear overhauser effect spectroscopy (NOESY) (Figure 3) spectrum, cross-peaks H-2/H$_3$-12, H-3/H$_3$-11, and H-8/H$_3$-11
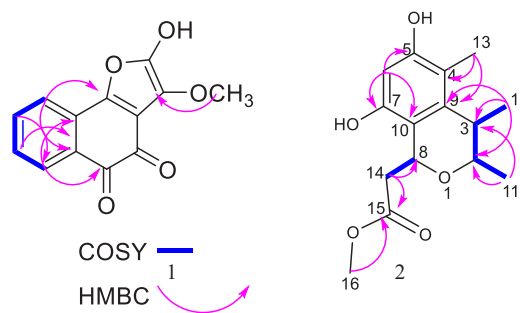

Figure 2. Key HMBC and COSY correlations of compounds 1 and 2.
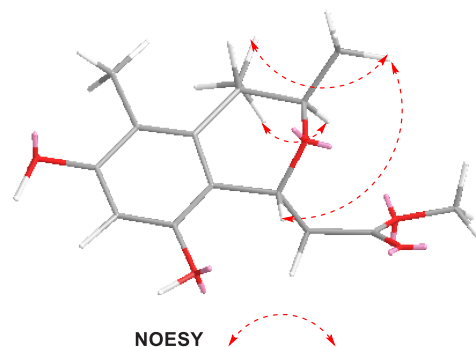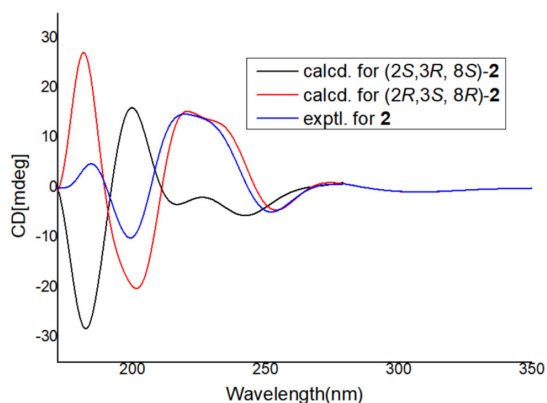

Figure 3. Key NOESY correlation of 2.

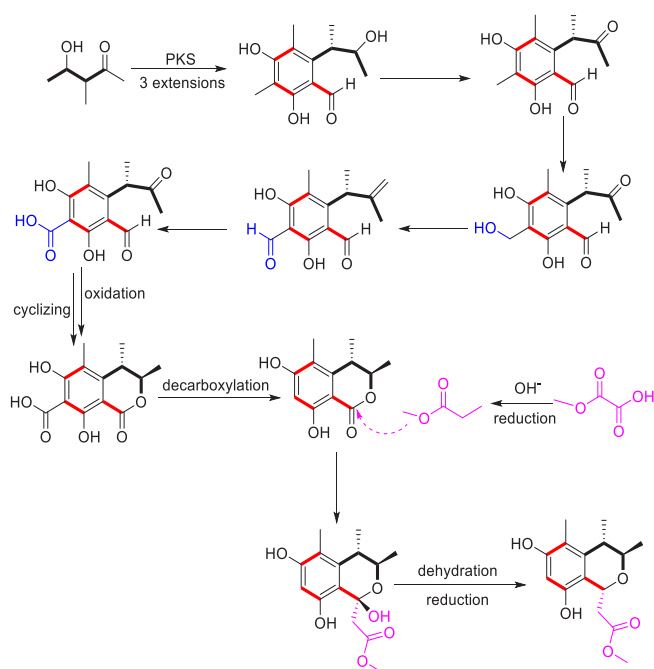**Figure 4.** Calculated and experimental ECD spectra of 2.

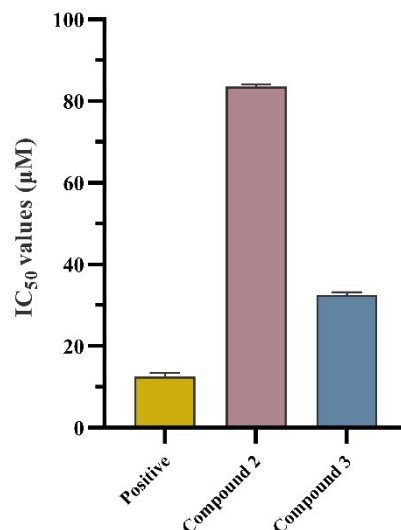**Figure 5.** Plausible biosynthetic pathway of compound 2.

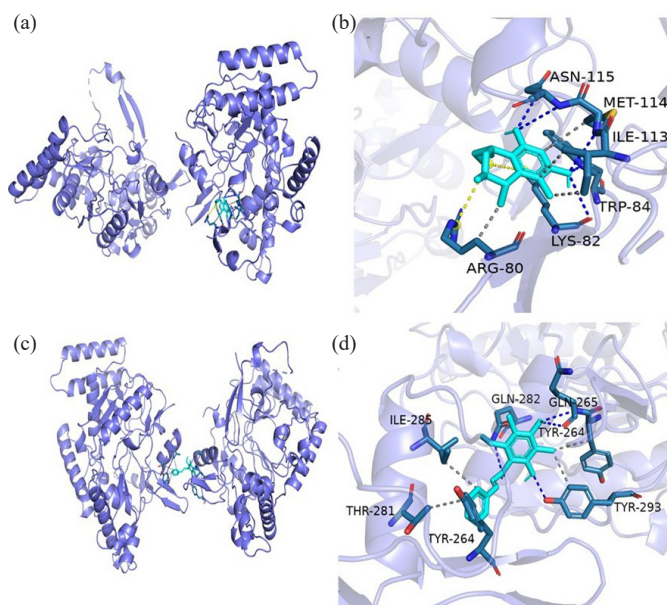**Figure 6.** Anti-inflammatory activities of compounds 2 and 3 (n=3). The values are represented by mean ± SD.

Figure 7. Molecular docking simulations of compounds (a, b) 2 and (c, d) 3.

were found, suggesting that Me-11, H-3, and H-8 were on the same side in **2**. The molecular structure of **2** was further determined as 2*R*, 3*S*, and 8*R* based on the calculated ECD spectra with its experimental values (Figure 4). Thus, the structure of **2** was elucidated.

Polyketide derivatives were specially found in plants and microorganisms. They are general biosynthetic precursors in the process of synthesizing aromatics. The biogenetic pathway of **2** is still unclear. Fortunately, successful heterologous expression of isocoumarin derivatives skeleton has been identified [22]. Therefore, we proposed the biosynthetic pathway of compound **2**, as shown in Figure 5.

In this study, ten known compounds were identified as 2, 4-dihydroxy-6-methoxy-3, 5-dimethylchalcone (**3**) [23], methyl ferulate (**4**) [24], 1-hydroxy-2,3,4-trimethoxydibenzofuran (**5**) [25], (+)-lyoniresmol (**6**) [26], isoliquiritigenin (**7**) [27], 3'-methoxydaidzein (**8**) [28], calycosin (**9**) [28], hydroxy-3-methoxy benzaldehyde (**10**) [29], 3-(4-hydroxy-3-methoxy-phenyl)-acrylic acid methoxycarbonyl methyl ester (**11**) [30], siderin (**12**) [31] based on the comparison of NMR information with those previously recorded in the papers.

3.2. Anti-inflammatory activity in-vitro

In bioassay experiments, the results showed that the IC_{50} of positive control was tested to be 12.5±0.97 μM. The IC_{50} values of compounds

2 and **3** for inhibition of NO production were 83.6±0.54 μM and 32.5±0.73 μM, respectively., as shown in Figure 6.

3.3. Molecular docking

For further studying the anti-inflammatory mechanism of compounds **2** and **3**, a molecular docking study was conducted based on the molecular interactions between **2, 3,** and iNOS. The iNOS (PDB ID:3E6T) was used as a target for molecular docking. Docking results displayed that the docking sites of compounds **2** and **3** (Figure 7) were well bound to their original sites. Compounds **2-3** interacted well with iNOS targets in their pockets. The binding free energy of compound **2** with 3E6T is -4.79 kcal/mol (Figure 7a and 7b). Compound **2** bounded to ASN115, LYS82, MET114, and TRP84 residues and formed four hydrogen bonds. Compound **2** formed non-polar hydrogen bonds with the TRP84, MET114, ARG80, and ILE113 residues. The binding free energy of compound **3** with 3E6T is -5.41 kcal/mol (Figure 7c and 7d), and it has hydrogen bonding interactions with residues GLN282,
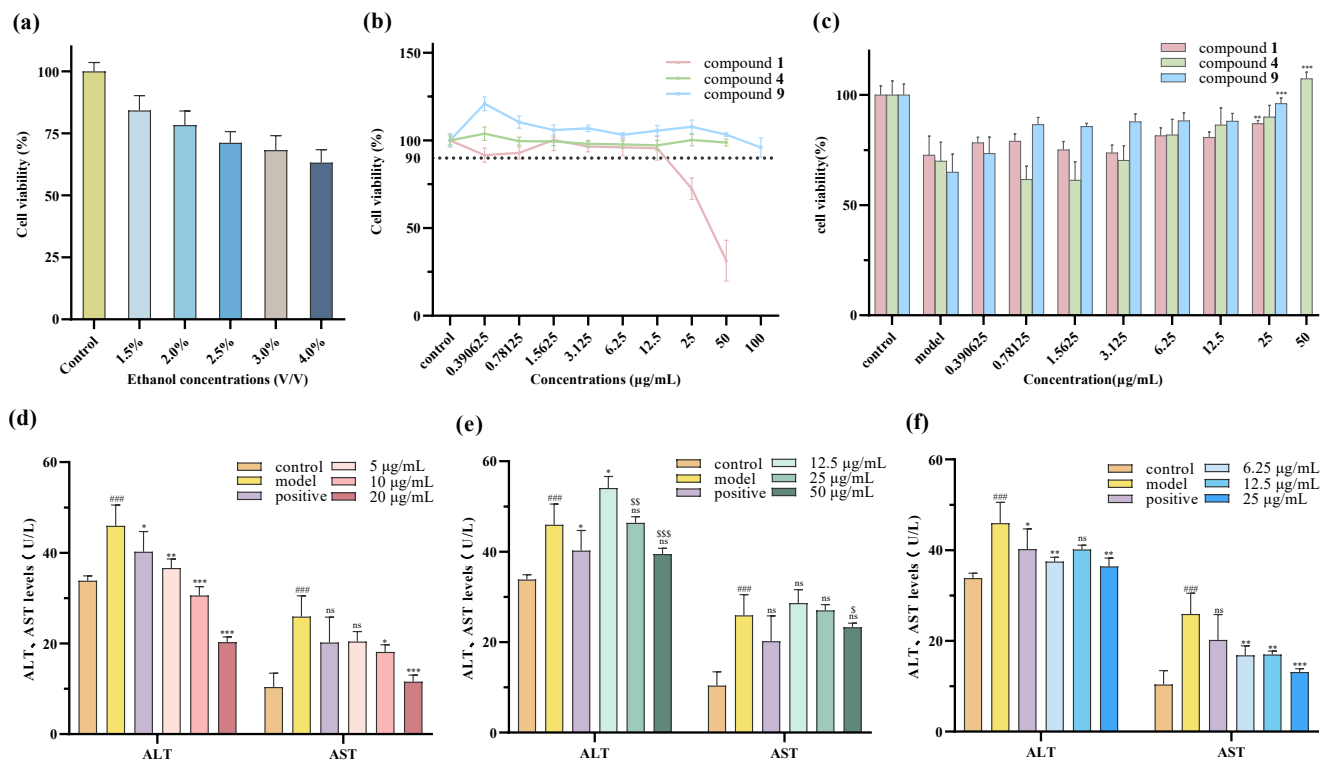
Figure 8. (a) Effects of different concentrations of ethanol (V/V) on L02 cell viability (n = 5, means ± SD). (b) Effect of different concentrations of compounds 1, 4, and 9 on the viability of L02 cells (n = 6, means ± SD). (c) Effects of different mass concentrations of compounds 1, 4, and 9 on alcohol-induced injury in L02 cells (n = 5, means ± SD). (d) ALT and AST levels of compound 1 (n = 3, means ± SD). (e) ALT and AST levels of compound 4 (n = 3, means ± SD). (f) ALT and AST levels of compound 9 (n = 3, means ± SD). Notes: Compared with the control group, # $p < 0.01$, ### $p < 0.001$; compared with the model group, * $p < 0.05$, ** $p < 0.01$, and *** $p < 0.001$; compared with low concentration of 4, \$, $p < 0.01$, \$\$, $p < 0.001$, \$\$\$, $p < 0.0001$.

GLN265, and TYR293, and non-polar interactions with residues TYR264, THR281, ILE285, and TYR293. Therefore, compounds **2** and **3** possess the potential to become lead drugs with anti-inflammatory activity.

3.4. Hepatoprotective activity in-vitro

In Figure 8(a), the cell viability rates at ethanol concentrations of 1.5%, 2%, 2.5%, 3%, and 4% (V/V) were determined to be 84.24 ± 6.00%, 78.40 ± 5.61%, 71.25 ± 4.51%, 68.25 ± 5.88%, and 63.22 ± 5.22%, respectively. Compared with the control group, ethanol intervention groups exhibited significant differences (P < 0.001). An ethanol concentration of 2.5% was ultimately selected, corresponding to a cell survival rate of approximately 71%, was ultimately selected as the modeling concentration for this experiment. As depicted in Figure 8(b), the appropriate concentrations of compounds **1**, **4**, and **9** were determined based on a criterion of a viability rate greater than 90%. Further research was performed to examine the significance of varying concentrations of these three compounds on alcohol-induced damage on L02 hepatocytes. As depicted in Figure 8(c), compared with the model group, both compound **1** and compound **9** showed increased cell viability in their treatment groups, reaching a maximum of 87% and 94%, respectively. Compound **4** also demonstrated cell proliferative activity with concentrations varying from 6.25 to 50 μg/mL. As shown in Figure 8(d-f), 2.5% ethanol stimulation significantly elevated the contents of ALT and AST in contrast with the control group (P < 0.001), indicating the alcohol-induced L02 cells injury model was established successfully. In comparison with the modeling group, compound **1** treatment groups at low, medium, and high concentrations (5, 10, 20 μg/mL) exhibited a concentration-dependent reduction in ALT and AST levels (Figure 8d). Similarly, the low, medium, and high (12.5, 25, 50 μg/mL) treatment groups of compound **4** showed a concentration-dependent decrease in ALT and AST levels, albeit the protective effect on ethanol-induced hepatocyte injury was no statistical significance (P > 0.05), as shown in Figure 8(e). Notably, the low and high

concentrations (6.25, 50 μg/mL) of compound **9** significantly reduced ALT and AST levels (P < 0.01), as shown in Figure 8(f). Based on these results, compounds **1,4** and **9** from LGS oral liquid can protect against liver cell damage induced by alcohol.

4. Conclusions

In summary, analysis of the chemical composition of LGS contributed to the identification of 12 compounds, including two new polyketide compounds (**1**, **2**). The structures of **1-12** were clarified by detailed NMR, HR-MS, and ECD calculations. Compounds **2** and **3** reduced the content of NO induced by LPS, with IC_{50} values of 83.6 ± 0.54 μM and 32.5 ± 0.73 μM, respectively. The optimal bioactivity evaluations and molecule docking results showed that compound **3** had the potential to be developed as a lead drug with anti-inflammatory activity. In addition, compounds **1**, **4,** and **9** alleviated alcohol-induced damage to human hepatic L02 cells and reduced the release of ALT and AST, indicating that these compounds possess good hepatoprotective activity for the treatment of ALD, which may have prospects for developing new drugs in the future. This also reveals a certain pharmacodynamic material basis for the antialcohol and liver-protective effects of the drink made from LGS. The bioactive components in the beverage await to be further discovered, and the related mechanisms need to be explored in depth.

CRediT authorship contribution statement

Mengyu Zhang: Performed the extraction, isolation and identification, and wrote the original draft. **Baorui Teng and Dan Zhang**: Accomplished the ECD calculation. **Xin Zhou:** Contributed to this work by bioassay experiments. **Xiujuan Fu, Siwei Chen, Sijing Liu, Zhi Li, Hui Lei:** Performed revised the manuscript. All authors have read and agreed to the published version of the manuscript.

Declaration of competing interest

The authors declare that they have no known competing financial interests or personal relationships that could have appeared to influence the work reported in this paper.

Declaration of Generative AI and AI-assisted technologies in the writing process

The authors confirm that there was no use of artificial intelligence (AI)-assisted technology for assisting in the writing or editing of the manuscript and no images were manipulated using AI.

Acknowledgment

Supplementary data

Supplementary material to this article can be found online at https://dx.doi.org/10.25259/AJC_37_2024.

References

1. Torruellas, C., French, S.W., Medici, V., 2014. Diagnosis of alcoholic liver disease. *World Journal of Gastroenterology*, **20**, 11684-11699. https://doi.org/10.3748/wjg.v20.i33.11684

2. Kumar, V., Sethi, B., Staller, D.W., Xin, X., Ma, J., Dong, Y., Talmon, G.A., Mahato, R.I., 2023. Anti-miR-96 and hh pathway inhibitor MDB5 synergistically ameliorate alcohol-associated liver injury in mice. *Biomaterials*, **295**, 122049. https://doi.org/10.1016/j.biomaterials.2023.122049

3. Nagy, L.E., 2015. The role of innate immunity in alcoholic liver disease. *Alcohol Research: Current Reviews*, **37**, 237-250.

4. Yang, K., Zhan, L., Lu, T., Zhou, C., Chen, X., Dong, Y., Lv, G., Chen, S., 2020. Dendrobium officinale polysaccharides protected against ethanol-induced acute liver injury *in-vivo* and *in-vitro* via the TLR4/NF-κB signaling pathway. *Cytokine*, **130**, 155058. https://doi.org/10.1016/j.cyto.2020.155058

5. Jiang, X.J., Pan, J.M., Ju, L.P., Zhang, J., Zhang, J.J., Zhuang, S.J., Xi, J.J., Zhuang, R.X., 2024. Establishment of liver cell injury model induced by different conditions *in-vitro*. *Modern Practical Medicine*, **36**, 154-8. https://doi.org/10.3969/j.issn.1671-0800.2024.03.004

6. Subramaniyan, V., Chakravarthi, S., Jegasothy, R., Seng, W.Y., Fuloria, N.K., Fuloria, S., Hazarika, I., Das, A., 2021. Alcohol-associated liver disease: A review on its pathophysiology, diagnosis and drug therapy. *Toxicology Reports*, **8**, 376-385. https://doi.org/10.1016/j.toxrep.2021.02.010

7. Dong, X.R., Chen, Q.Q., Xue, M.L., Wang, L., Wu, Q., Luo, T.F., 2023. Effect of polyene phosphatidylcholine/ursodeoxycholic acid/ademetionine on pregnancy outcomes in intrahepatic cholestasis. *World Journal of Clinical Cases*, **11**, 6431-9. https://doi.org/10.12998/wjcc.v11.i27.6431

8. Spina, D., Page, C.P., 2017. Xanthines and phosphodiesterase inhibitors. *Handbook of Experimental Pharmacology*, **237**, 63-91. https://doi.org/10.1007/164_2016_71

9. Oray, M., Abu Samra, K., Ebrahimiadib, N., Meese, H., Foster, C.S., 2016. Long-term side effects of glucocorticoids. *Expert Opinion on Drug Safety*, **15**, 457-465. https://doi.org/10.1517/14740338.2016.1140743

10. Dhooria, S., Sehgal, I.S., Agarwal, R., Muthu, V., Prasad, K.T., Dogra, P., Debi, U., Garg, M., Bal, A., Gupta, N., Aggarwal, A.N., 2023. High-dose (40 mg) *versus* low-dose (20 mg) prednisolone for treating sarcoidosis: A randomised trial (SARCORT trial). *European Respiratory Journal*, **62**, 2300198. https://doi.org/10.1183/13993003.00198-2023

11. Ren, K.L., Fan, R.Y., Shi, Y.H., Zhang, Y., Guo, J.H., Liu, Y.L., 2025. Research progress on the alleviation of alcoholic liver injury by natural product active ingredients. *The Journal of Medical Theory and Practice*, 38, 576-578+582. https://doi.org/10.19381/j.issn.1001-7585.2025.04.009

12. Dong, L., Zhang, H.T., Kang, Y.Y., Wang, F., Guo, H.L., Dong, Y., Dong Lu, Zhang Haotian, Kang Yanyu, Wang Fei, Guo Haolin, Dong Ying, Yang Yong, Bai Ting, 2025. Effects of chrysin on the intestinal flora in mice with alcoholic liver disease model. *Her Med.*, 44, 176-182. https://doi.org/10.3870/j.issn.1004-0781.2025.02.002

13. Xiang, Q., Zhang, G.T., Lu, R.Q., Tang, J.W., He, S.Q., Min, C., Geng, J.Z., 2024. Research progress on the alleviation of alcoholic liver injury based on bibliometric analysis of medicinal and food homologous substances. *Science and Technology of Food Industry*, **45**, 1-11. https://doi.org/10.13386/j.issn1002-0306.2023060041

14. Hou, Y., Liu, Y.-P., Li, Z., Li, B., Yang, G.-C., Wei, M., 2018. Mechanisms for zhige oral solution to prevent and treat alcoholic liver disease in rats. *World Chinese Journal of Digestology*, **26**, 296-304. https://doi.org/10.11569/wcjd.v26.i5.296

15. Chen, M.L., Wang, X.D., Li, B., Liu, Y., Lei, D., Wei, M., 2020. Zhige oral liquid regulates glucose and lipid metabolism in rats with alcoholic liver disease through AMPK/SREBP-1/Lipin-1. Lishizhen Med Mat Med Res. **31**, 1080-4. https://doi.org/10.3969/j.issn.1008-0805.2020.05.015

16. Wei, S., Li, M., Zhao, L., Wang, T., Wu, K., Yang, J., Tang, M., Zhao, Y., Shen, J., Du, F., Chen, Y., Deng, S., Xiao, Z., Wei, M., Li, Z., Wu, X., 2024. Fingerprint profiling for quality evaluation and the related biological activity analysis of polysaccharides from liuweizhiji gegen-sangshen beverage. *Frontiers in nutrition*, **11**, 1431518. https://doi.org/10.3389/fnut.2024.1431518

17. Gou, S.S., Huang, X.P., Li, B., Wang, X.D., Huang, S., Wei, M., 2023. Mechanism of Zhige Oral Liquid in Preventing and Treating Alcoholic Liver Injury Through Syk/Ras/ERK Signal Pathway. *Journal of Traditional Chinese Medical Sciences*, **35**, 1560-5. http://doi:10.16448/j.cjtcm.2023.0823

18. Wei, S., Jiang, Y., Li, M., Zhao, L., Wang, T., Wei, M., Zhao, Q., Zeng, J., Zhao, Y., Shen, J., Du, F., Chen, Y., Deng, S., Xiao, Z., Li, Z., Wu, X., 2024. Chemical profiling and quality evaluation of liuweizhiji gegen-sangshen oral liquid by UPLC-q-TOF-MS and HPLC-diode array detector fingerprinting. *Phytochemical analysis: PCA*, **35**, 860-872. https://doi.org/10.1002/pca.3333

19. Jiang, P., Luo, J., Jiang, Y., Zhang, L., Jiang, L., Teng, B., Niu, H., Zhang, D., Lei, H., 2022. Anti-inflammatory polyketide derivatives from the sponge-derived fungus *pestalotiopsis* sp. SWMU-WZ04-2. *Marine Drugs*, **20**, 711. https://doi.org/10.3390/md20110711

20. Trott, O., Olson, A.J., 2010. AutoDock vina: Improving the speed and accuracy of docking with a new scoring function, efficient optimization, and multithreading. *Journal of Computational Chemistry*, **31**, 455-461. https://doi.org/10.1002/jcc.21334

21. Laskowski, R.A., Swindells, M.B., 2011. LigPlot+: Multiple ligand-protein interaction diagrams for drug discovery. *Journal of Chemical Information and Modeling*, **51**, 2778-2786. https://doi.org/10.1021/ci200227u

22. Tammam, M.A., Gamal El-Din, M.I., Abood, A., El-Demerdash, A., 2023. Recent advances in the discovery, biosynthesis, and therapeutic potential of isocoumarins derived from fungi: A comprehensive update. *RSC Advances*, **13**, 8049-8089. https://doi.org/10.1039/d2ra08245d

23. DellaGreca, M., Fiorentino, A., Izzo, A., Napoli, F., Purcaro, R., Zarrelli, A., 2007. Phytotoxicity of secondary metabolites from aptenia cordifolia. *Chemistry & Biodiversity*, **4**, 118-128. https://doi.org/10.1002/cbdv.200790016

24. Phuong, N.T., Cuong, T.T., Quang, D.N., 2014. Anti-inflammatory activity of methyl ferulate isolated from stemona tuberosa lour. *Asian Pacific journal of tropical Medicine*, **7S1**, S327-S331. https://doi.org/10.1016/S1995-7645(14)60254-6

25. Wang, Y., Lang, L.J., Zhu, Q.J., Wu, X.R., Shen, L., Jiang, B., Xiao, C.J., 2022. Dibenzofurans from crataegus oresbia and their lipid-lowering activity. *Natural Product Research*, **36**, 6297-6303. https://doi.org/10.1080/14786419.2022.2036146

26. Kaneda, N., Kinghorn, A.D., Farnsworth, N.R., Tuchinda, P., Udchachon, J., Santisuki, T., Reutrakul, V., 1990. Two diarylheptanoids and a lignan from Casuarina junghuhniana. *Phytochemistry*, **29**, 3366-8. https://doi.org/10.1016/0031-9422(90)80220-b

27. Yahara, S., Ogata, T., Saijo, R., Konishi, R., Yamahara, J., Miyahara, K., Nohara, T., 1989. Isoflavan and related compounds from Dalbergia odorifera. I. *Chemical and Pharmaceutical Bulletin*, **37**, 979-987. https://doi.org/10.1248/cpb.37.979

28. Takai, M.A.K.O.T.O., Yamaguchi, H.I.S.A.S.H.I., Saitoh, T.A.M.O.T.S.U., Shibata, S.H.O.J.I., 1972. Chemical studies on the oriental plant drugs XXXV the chemical constituents of the heartwood of *maackia amurensis* var. buergeri. *Chemical and Pharmaceutical Bulletin*, **20**, 2488-2490. https://doi.org/10.1248/cpb.20.2488

29. Kamaal, S., Faizi, M.S.H., Ali, A., Ahmad, M., Gupta, M., Dege, N., Iskenderov, T., 2019. Crystal structure of 4-[(2-hydroxy-3-methoxybenzyl)amino]benzoic acid hemihydrate. *Acta Crystallographica Section E Crystallographic Communications*, **75**, 159-162. https://doi.org/10.1107/s2056989018018455

30. Reddy, K.K., Shanker, K.S., Ravinder, T., Prasad, R.B.N., Kanjilal, S., 2010. Chemo-enzymatic synthesis and evaluation of novel structured phenolic lipids as potential lipophilic antioxidants. *European Journal of Lipid Science and Technology*, **112**, 600-8. https://doi.org/10.1002/ejlt.200900200

31. Xuan, L.I.U., 2012. Chemical constituents from *imperata cylindrica*. *China Journal of Chinese Materia Medica*. https://doi.org/10.4268/cjcmm20121523